粘性尾流之渦流運動預測模式

A Model for Predicting Vortex Motion in a Viscous Wake

淡江大學水利系教授

曾　振　遠*

Cheng-yuan Tseng

摘　　要

尾流 (Wake) 形成之主要機構原理尚未被透徹了解，旋渦 (Vortex) 受粘性 (Viscosity) 之影響其流函數 (Stream function) 尚無解析解，因此粘性尾流 (Viscous wake) 仍是現代流體專家探討專題之一，本文主要構建粘性尾流之渦流運動 (Vortex motion) 預測模式，其輸入資料僅需圓柱直徑、雷諾數 (Reynolds number 及史戴荷數 (Strouhal number)，結果顯示第一個旋渦之核心半徑幾近於水流於圓柱分離點之邊界層厚度，而與 1986 年 Wei 與 Smith 之假說相映。實驗亦證實粘性尾流中之旋渦係由四個在分離線 (Separation line) 形成之副旋渦 (Secondary vortex) 配對結合而成，首度使尾流形成主因有合理性解釋是爲本文之貢獻。依時間之變化本模式可測單一旋渦之核心半徑及速度剖面，亦可推測第 n 個旋渦强度與極大速度。在應用方面，易於以線性疊加 (Superposition) 計算粘性尾流中無限多旋渦之速度場。經與理想流之速度場比較，顯示粘性之影響使旋渦核心之速度由理想尾流 (Potential wake) 之無限大改變爲趨近於零較符實際現象。本研究之初步成果顯著，尚待繼續。

ABSTRACT

The results of the model has shown that the radius of the first shed vortex core is nearly equal to the boundary layer thickness at the separation point of the cylinder. Research at Albrook Hydraulic Laboratory has shown that the initiation of Strouhal vortex is due to the pairing of four secondary vortexes. A numerical model predicting the maximum velocity, core radius, tangential velocity profile, and strength of the *n*th vortex behind a circular cylinder has been developed. As input, this model requires the characteristics of the viscous wake as well as the Strouhal and Reynolds numbers associated with the flow arround the cylinder. By superposing the velocity components of infinite vortexes in the wake, the velocity field has been analyzed. Comparison of the velocity field for both viscous and potential wakes are good, with some variance existing in the velocity distribution in the viscous core.

* Professor, Department of Hydraulic Engineering, Tamkang University, Taiwan, Republic of China. Completed while on leave at Department of Civil and Environment Engineering, Washington State University. The author wants to thank Dr. Walter C. Mih for financial support and supervision during the research.

1. Introduction

The phenomenon of vortex motion in a potential wake behind a cylinder has been analyzed since 1912 (Karman and Ruback, 1912). For a viscous wake, a combined vortex, or Rankine vortex (Rankine, 1858) which has a solid rotation at the core, has been proposed instead of the potential vortex in the wake by Hooker (1936) and Schaefer and Eskinazi (1959). However, Hooker considered only one viscous vortex while all the others remained potential vortexes. Schaefer and Eskinazi expressed a summation of infinite viscous votexes in terms of time, kinematic viscosity, and the frequency of vortex shedding.

This paper has developed a model which is in terms of the Strouhal number, the Reynolds number, the diameter of cylinder, and the order number, n, of the nth vortex in the wake for predicting the vortex motion. The results of the model have been compared with the Schaefer and Eskinazi experimental data and have proven its validity. Applying the model, the velocity field has been satisfactorily generated through the computer simulation. The only difference between the viscous and potential wakes are bound in the velocities of the vortex core.

The model has reasonably described the phenomenon of the initiation of the vortex shedding behind a cylinder, showing that the first shed vortex is due to the pairing of many small vortexes which are generated by the boundary layer flow along the separation line. This description has been observed in Albrook Laboratory at Washington State University, and agrees well with the hypothesis of Wei and Smith (1986) who did not use any mathematical expression.

The objective of this paper is to demonstrate the suitability, sufficiency, and applicableness of the model. The application and the analysis needs to be extended, as much work remains to be done.

2. Theoretical Consideration of a Viscous Vortex

For two dimensional viscous vortex motion, the vorticity diffusion equation is

$$\frac{\partial \zeta}{\partial t} = \nu\left(\frac{\partial^2 \zeta}{\partial r^2} + \frac{1}{r}\frac{\partial \zeta}{\partial r}\right) \qquad (2.1)$$

The solution of Eq. (2.1) is (Oseen, 1911; Lamb, 1932)

$$\zeta(r, t) = \frac{\Gamma_0}{4\pi\nu t}\exp\left(-\frac{r^2}{4\nu t}\right) \qquad (2.2)$$

where

ζ= vorticity

Γ_0 = circulation of the original vortex filament

ν = kinematic viscosity of the fluid

t= time after the vortex shedding from the cylinder or age of a particular vortex in the wake

r= distance from a point to the vortex center

The circulation, or the total vorticity enclosed by a circle of radius, r, is

$$\Gamma = \int_0^r 2\pi r\zeta dr = \Gamma_0\left(1 - \exp\left(-\frac{r^2}{4\nu t}\right)\right) \qquad (2.3)$$

The circumferential velocity v_θ at time t and radius r is

$$v_\theta = \frac{\Gamma}{2\pi r} = \frac{\Gamma_0}{2\pi r}\left(1 - \exp\left(-\frac{r^2}{4\nu t}\right)\right) \qquad (2.4)$$

The maximum velocity v_m occurs at r_m, and can be obtained from Eq. (2.4) (Schaefer and Eskinazi, 1959; Odgaar, 1986) by

$$r_m^2 = 5\nu t \tag{2.5}$$

and

$$v_m = \frac{1}{1.4}\frac{\Gamma_0}{2\pi r_m} \tag{2.6}$$

Substituting Eqs (2.5) and (2.6) into Eq (2.4), the velocity, v_θ, and the dimensionless expression of v_θ/v_m are

$$v_\theta = \frac{\Gamma_0}{2\pi r}\left(1 - \exp\left(-1.25\left(\frac{r}{r_m}\right)^2\right)\right) \tag{2.7}$$

$$\frac{v_\theta}{v_m} = 1.4\frac{r_m}{r}\left(1 - \exp\left(-1.25\left(\frac{r}{r_m}\right)^2\right)\right) \tag{2.8}$$

For a free vortex, $v_\theta = \frac{\Gamma_0}{2\pi r}$, dividing by Eq (2.6) yeields

$$\frac{v_\theta}{v_m} = 1.4\frac{r}{r_m} \tag{2.9}$$

For a forced vortex, expanding the bracked term of Eq (2.8) as a power series and cancelling the higher order terms yields

$$\frac{v_\theta}{v_m} = 1.4\frac{r_m}{r}\left\{1 - \left(1 - 1.25\left(\frac{r}{r_m}\right)^2 + \ldots\right)\right\}$$

$$\frac{v_\theta}{v_m} = 1.75\frac{r}{r_m} \tag{2.10}$$

The comparison of a Rankine vortex and the free vortex is shown in Fig 1.

3. The Model for Predicting the Viscous Core

In the viscous wake, the radius of vortex core, r_m is changing with the distance from the cylinder or with the time after shedding according to Eq. (2.5). If the frequency of vortex shedding from

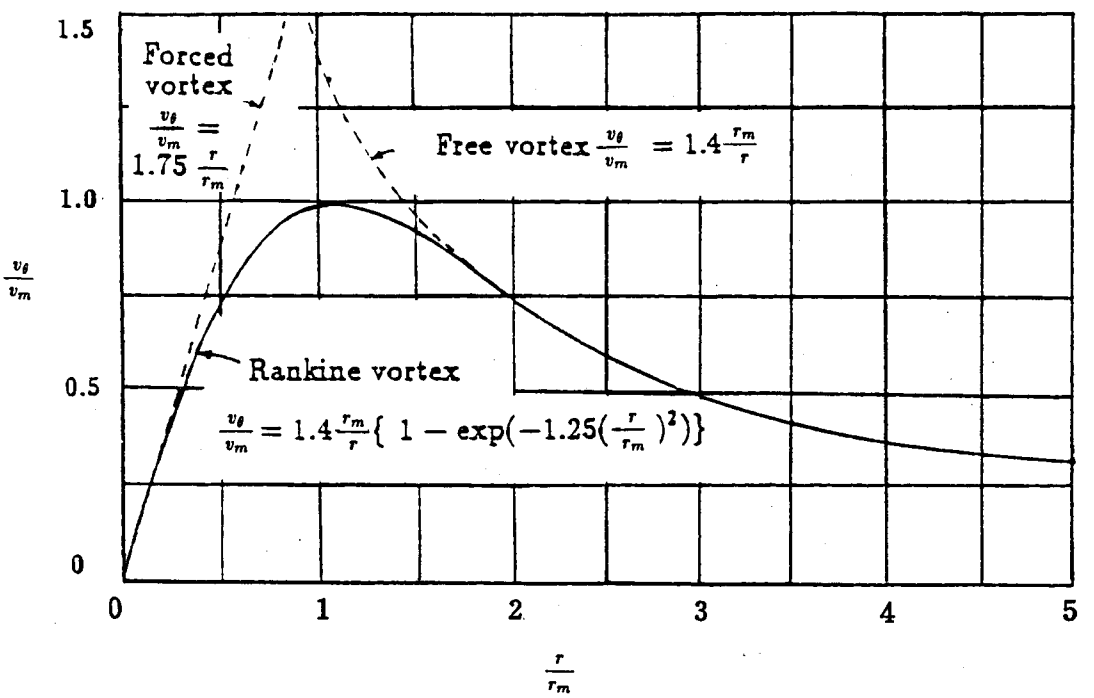

Figure 1. The comparison of Rankine vortex and free vortex

one side of the cylinder is defined as f, then the time period of shedding is $T = \frac{1}{f}$. The age of the nth vortex, t, may be expressed in terms of the period T and the number n of the shed vortex in the wake as $t = nT$. Eq. (2.5) can be rewritten as

$$r_m^{(n)} = \sqrt{5\nu nT} \qquad (3.1)$$

From the Strouhal number and Reynolds number, $S = \frac{d}{UT}$ and $R = \frac{Ud}{\nu}$, T and ν can be expressed by

$$T = \frac{d}{US} \qquad (3.2)$$

and

$$\nu = \frac{Ud}{R} \qquad (3.3)$$

From Eqs (3.2) and (3.3), the product of Strouhal number and Reynolds number is

$$SR = \frac{d^2}{T\nu} \qquad (3.4)$$

Substituting Eqs (3.2) and (3.3) into Eq. (3.1), yields

$$r_m^{(n)} = \sqrt{\frac{5nd^2}{SR}} \qquad (3.5)$$

If the flow conditions, S, R, and the diameter of cylinder, are given, Eq. (3.5) may be used to predict the core radius of nth vortex.

In general, n takes on integer values, $n = 1, 2, 3, \ldots$, to designate sequential vortexes in the wake. The ratio of the radius of nth vortex, $r_m^{(n)}$, to the diameter of the cylinder is

$$\frac{r_m^{(n)}}{d} = \sqrt{\frac{5n}{SR}} \qquad (3.6)$$

The vortex at the time of shedding from the cylinder is designated as n = 1 and the core radius, $r_m^{(1)}$, is

$$\frac{r_m^{(1)}}{d} = \sqrt{\frac{5}{SR}} \qquad (3.7)$$

The core radius of the nth vortex is proportional to the radius of the first vortex. The proportion constant is $\sqrt{n}$, i. e.

$$r_m^{(n)} = r_m^{(1)}\sqrt{n} \qquad (3.8)$$

If the core radius of the first vortex behind the cylinder is given, the nth vortex can be predicted by Eq. (3.8).

Eqs (2.6) and (2.7) may be rewritten as

$$v_m^{(n)} = \frac{1}{1.4}\frac{\Gamma_0}{2\pi r_m^{(n)}} \qquad (3.9)$$

$$v_\theta^{(n)} = \frac{\Gamma_0}{2\pi r}\left(1 - \exp\left(-1.25\left(\frac{r}{r_m^{(n)}}\right)^2\right)\right) \qquad (3.10)$$

The maximum velocity, $v_m^{(n)}$, and the tangential velocity, $v_\theta^{(n)}$, of the nth vortex can be expressed in the following dimensionless form.

$$\frac{v_m^{(n)}d}{\Gamma_0} = \frac{1}{1.4}\frac{\sqrt{SR}}{2\pi\sqrt{5n}} = 0.05\left(\frac{SR}{n}\right)^{\frac{1}{2}} \qquad (3.11)$$

$$\frac{v_\theta^{(n)}d}{\Gamma_0} = \frac{1}{2\pi}\left(\frac{d}{r}\right)\left(1 - e^{-\frac{SR}{4n}\left(\frac{r}{d}\right)^2}\right) \qquad (3.12)$$

Eq. (3.12) is a general equation which completely describes the vortex motion of the nth vortex in the wake. From Eqs (2.3) and (3.4), the circulation of nth vortex is

$$\Gamma_n = \Gamma_0\left(1 - e^{-\frac{SR}{4n}\left(\frac{r}{d}\right)^2}\right) \qquad (3.13)$$

4. The Comparison of the Model with Schaefer and Eskinazi Experiment data

The experiment data of the Shaefer and Eskinazi tests are shown in Table 1.

Table 1. The experimental data of Schaefer and Eskinazi test (1959)

R	$\frac{x}{d}$	$\frac{r_m}{d}$	$\frac{h}{d}$	$\frac{h}{l}$
62	3	0.51	0.80	0.12
62	4	0.59	0.48	0.07
62	5	0.65	0.52	0.08
62	6	0.72	0.84	0.13
62	7	0.78	0.96	0.15
62	8	0.83	1.14	0.18
62	10	0.93	1.28	0.20
62	12	1.01	1.98	0.30
62	15	1.12	1.82	0.28
62	20	1.31	2.00	0.31
62	25	1.46	1.42	0.22
94	2	0.36	0.70	0.13
94	3	0.44	0.52	0.10
94	4	0.51	0.80	0.15
94	5	0.57	1.04	0.19
94	6	0.63	1.18	0.22
94	7	0.68	1.26	0.23
94	8	0.72	1.30	0.24
94	10	0.81	1.20	0.22
94	12	0.88	1.16	0.22
94	15	0.98	1.06	0.20
94	20	1.14	0.90	0.18
118	5	0.50	1.34	0.27
118	7	0.60	1.20	0.24
118	10	0.71	1.00	0.20
118	15	0.87	0.32	0.06

First test: R = 62, S = 0.14

In the Table 1, while $\frac{x}{d} = 6$, $\frac{r_m}{d} = 0.72$, $\frac{h}{d} = 0.84$, and $\frac{h}{l} = 0.13$. Hence,

$$\frac{l}{d} = \frac{\frac{h}{d}}{\frac{h}{l}} = \frac{0.84}{0.13} = 6.46$$

$$l = 6.46d$$

This data shows that: the first vortex is at $\frac{x}{d} = 6.46 \approx 6$, the second vortex is at $\frac{x}{d} = 12.92 \approx 12$, and the third vortex is at $\frac{x}{d} = 19.38 \approx 20$. From Eq. (3.7),

$$\frac{r_m^{(1)}}{d} = \sqrt{\frac{5}{0.14 \times 62}} = 0.75$$

The values, $\frac{r_m}{d}$ and $\frac{r_m^{(1)}}{d}$, are almost same.

The experimental data of the ratios of vortex (2) or (3) to vortex (1) are shown as follows:

Vortex No.	$\frac{x}{d}$	$\frac{r_m}{d}$	measured	predicted $\sqrt{n}$
(1)	6	0.72		
(2)	12	1.10	$\frac{r_m^{(2)}}{r_m^{(1)}} = 1.402$	$\sqrt{2} = 1.414$
(3)	20	1.31	$\frac{r_m^{(3)}}{r_m^{(1)}} = 1.819$	$\sqrt{3} = 1.732$

Second test: R = 94, S = 0.16

In the Table 1, while $\frac{x}{d} = 5$, $\frac{r_m}{d} = 0.57$, $\frac{h}{d} = 1.04$, and $\frac{h}{l} = 0.19$. Hence,

$$\frac{l}{d} = \frac{\frac{h}{d}}{\frac{h}{l}} = \frac{1.04}{0.19} = 5.47$$

$$l = 5.47d$$

This data shows that: the first vortex is at $\frac{x}{d} = 5.47 \approx 5$, the second vortex is at $\frac{x}{d} = 10.94 \approx 10$, and the third vortex is at $\frac{x}{d} = 16.41 \approx 15$. From Eq. (3.7),

$$\frac{r_m^{(1)}}{d} = \sqrt{\frac{5}{0.16 \times 94}} = 0.57$$

The values, $\frac{r_m}{d}$ and $\frac{r_m^{(1)}}{d}$, are almost same.

The experimental data of the ratios of vortex (2) or (3) to vortex (1) are shown as follows:

Vortex No.	$\frac{x}{d}$	$\frac{r_m}{d}$	measured	predicted $\sqrt{n}$
(1)	5	0.57		
(2)	10	0.81	$\frac{r_m^{(2)}}{r_m^{(1)}} = 1.421$	$\sqrt{2} = 1.414$
(3)	15	0.98	$\frac{r_m^{(3)}}{r_m^{(1)}} = 1.719$	$\sqrt{3} = 1.732$

Third test: R = 118, S = 0.17

In the Table 1, while $\frac{x}{d} = 5$, $\frac{r_m}{d} = 0.50$, $\frac{h}{d} = 1.34$, and $\frac{h}{l} = 0.27$. Hence,

$$\frac{l}{d} = \frac{\frac{h}{d}}{\frac{h}{l}} = \frac{1.34}{0.27} = 4.96$$

$$l = 4.96d$$

This data shows that: the first vortex is at $\frac{x}{d} = 4.96 \approx 5$, the second vortex is at $\frac{x}{d} = 9.92 \approx 10$, and the third vortex is at $\frac{x}{d} = 14.88 \approx 15$. From Eq. (3.7),

$$\frac{r_m^{(1)}}{d} = \sqrt{\frac{5}{0.17 \times 118}} = 0.50$$

The values, $\frac{r_m}{d}$ and $\frac{r_m^{(1)}}{d}$, are almost same.

The experimental data of the ratios of vortex (2) or (3) to vortex (1) are shown as follows:

Vortex No.	$\frac{x}{d}$	$\frac{r_m}{d}$	Measured	predicted $\sqrt{n}$
(1)	5	0.50		
(2)	10	0.71	$\frac{r_m^{(2)}}{r_m^{(1)}} = 1.420$	$\sqrt{2} = 1.414$
(3)	15	0.87	$\frac{r_m^{(3)}}{r_m^{(1)}} = 1.740$	$\sqrt{3} = 1.732$

The results of the experiment data are in close agreement with the values predicted using the model in different Reynolds numbers.

5. The Model for Predicting the Velocity Field in the Viscous Wake

5.1 The configuration of the flow field

An uniform flow with velocity U passing over a cylinder is considered to be the flow field of the model. If the Reynolds number is greater than 40 (Roshko, 1954), the flow field can be classified three typical regions; formation, stable, and decay region (Schaefer and Eskinazi, 1959). In the formation region, the flow separates from the cylinder, in which, the secondary vortexes are formed and combined into a Strouhal vortex (Wei and Smith, 1986). At the beginning of the stable region, the first vortex starts moving to the wake. Prior to the decay region, the vortexes become depressed and disappear. This model only predicts the velocity field in the stable region.

In the stable region, it has been

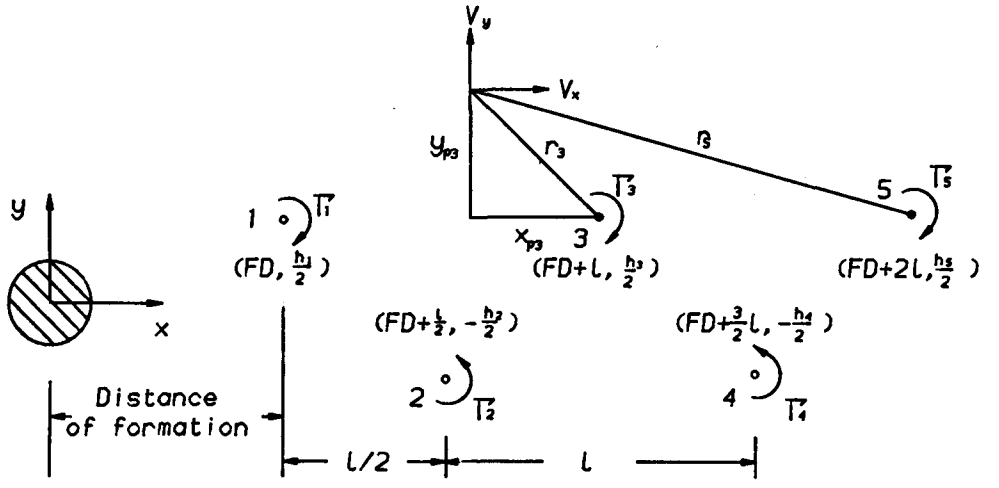

Figure 2. The flow field and the coordinate system

observed and proven that a staggered arrangement known as the Karman vortex street is formed (Karman and Ruback, 1912). This is as shown in Fig. 2. The number of vortexes in the street are denoted as odd numbers (1,3,5,...) for the first row, and as even numbers (2,4,6,...) for the second row. The length of the longitudinal separation of two vortexes in one row is assumed a constant, l (Roshko, 1954; Bloor and Gerrard, 1966). The transverse separation of two rows, h_n, are varied with respect to nth vortex. In this model the h_n is assumed as an average value of the experimental data in order to compare with the results of potential wake. The shedding frequency of vortex is f, and the time period between two shed vortexes is T.

The coordinate system is choosen as shown in Fig 5.1. The origin is located at the center of the circular cylinder. The distance of the formation region is designated as FD which is an uninfluenced variable to the model since it will be cancelled during difference operations. The coordinates of vortex centers in the first row are $(FD, \frac{h_1}{2})$, $(FD + l, \frac{h_3}{2})$, . . . $(FD + \frac{(k-1)}{2}l, \frac{h_k}{2})$, . . . Similarly. those in the second row are $(FD + \frac{l}{2}, -\frac{h_2}{2})$, . . . $(FD + \frac{k}{2}l, -\frac{h_{k+1}}{2})$, . . .

The circulations of the vortexes, or vortex strength, are designated as negative, or clockwise, in the first row and positive, or counterclockwise, in the second row. In this model, the strength of the first vortex, Γ_0, is calculated as a potential vortex which is (Karman, 1912)

$$\Gamma_0 = \frac{2u_c l}{\tanh \frac{\pi h}{l}} \qquad (5.1)$$

where $\frac{h}{l} = 0.281$, u_c is the velocity of vortex center, or $u_c = U - \frac{l}{T}$. From Eq (3.13), the circulation of nth vortex is

$$\Gamma_n = \Gamma_0(1 - e^{-\frac{SR}{4n}(\frac{r}{d})^2}) \qquad (5.1a)$$

5.2 Algorithm of the computation

1. Calculating the distances of point P to kth vortex center

The coordinate of any point P in the flow field is given as (x,y). r_{Pk} and y_{Pk} are the X and Y components of the distance, r_k, from point P to kth vortex center. They can be expressed as

$$x_{Pk} = x - (FD + (\frac{k-1}{2})l)$$

$$y_{Pk} = y - (-1)^{k-1}\frac{h_k}{2}$$

and

$$r_k = \sqrt{(x_{Pk})^2 + (y_{Pk})^2} \qquad (5.2)$$

2. Calculating the X and Y components of circumferencial velocity

From Eq (3.12) and changing the n to $\frac{k+1}{2}$, the circumferencial velocity of point P refer to kth vortex is

$$\frac{v_\theta d}{\Gamma_0} = \frac{(-1)^k}{2\pi}(\frac{d}{r_k})(1 - e^{-\frac{SR}{2(k+1)}(\frac{r_k}{d})^2}) \qquad (5.3)$$

The X and Y components of v_θ, which are $v_x k$ and $v_y k$ respectively, are

$$v_{xk} = -\frac{\Gamma_0}{d}\frac{(-1)^k}{2\pi}(\frac{d}{r_k})(1 - e^{-\frac{SR}{2(k+1)}(\frac{r_k}{d})^2})\frac{y_{Pk}}{r_k} \qquad (5.4a)$$

$$v_{yk} = \frac{\Gamma_0}{d}\frac{(-1)^k}{2\pi}(\frac{d}{r_k})(1 - e^{-\frac{SR}{2(k+1)}(\frac{r_k}{d})^2})\frac{x_{Pk}}{r_k} \qquad (5.4b)$$

3. Taking the summation of the circumferencial velocity components of point P

The velocity components of point P refer to the free stream, V_x and V_y, are taking the superposition of the velocity components of v_θ with respect to kth vortex, hence

$$V_x = \sum_{k=1}^{\infty} v_{xk}$$

$$= \sum_{k=1}^{\infty} -\frac{\Gamma_0}{d}\frac{(-1)^k}{2\pi}\left(\frac{d}{r_k}\right)\left(1 - e^{-\frac{SR}{2(k+1)}\left(\frac{r_k}{d}\right)^2}\right)\frac{y_{Pk}}{r_k} \tag{5.5a}$$

$$V_y = \sum_{k=1}^{\infty} v_{yk}$$

$$= \sum_{k=1}^{\infty} \frac{\Gamma_0}{d}\frac{(-1)^k}{2\pi}\left(\frac{d}{r_k}\right)\left(1 - e^{-\frac{SR}{2(k+1)}\left(\frac{r_k}{d}\right)^2}\right)\frac{x_{Pk}}{r_k} \tag{5.5b}$$

The dimensionless forms are

$$\frac{V_x d}{\Gamma_0} = \sum_{k=1}^{\infty} -\frac{(-1)^k}{2\pi}\left(\frac{d}{r_k}\right)\left(1 - e^{-\frac{SR}{2(k+1)}\left(\frac{r_k}{d}\right)^2}\right)\frac{y_{Pk}}{r_k} \tag{5.6a}$$

$$\frac{V_y d}{\Gamma_0} = \sum_{k=1}^{\infty} \frac{(-1)^k}{2\pi}\left(\frac{d}{r_k}\right)\left(1 - e^{-\frac{SR}{2(k+1)}\left(\frac{r_k}{d}\right)^2}\right)\frac{x_{Pk}}{r_k} \tag{5.6b}$$

5.3 Results of the velocity field

In the model the Strouhal number, the Reynolds number, the time period, and the row separation were obtained from the experimental data. The tests were done in a 3 foot wide water flume with the 1.25 inch diameter test cylinder placed on the center line of the flume. The cylinder extended from the flume bottom to above the water surface. The water depth was 12 inches. Dye was released near the water surface. For one free stream velocity U, the tests at two diameter intervals measured the average time period, the velocity of vortex center relative to the cylinder, and the row separation. Using these data, the computer program calculated the Strouhal number, the Reynolds number, the longitudinal separation, and the circulation.

The test results are shown in Table 2. Column 1 shows the locations. Columns 2 and 3 show the frequency and Strouhal number. The velocity of vortex center referring to the free stream, u_c, was calculated by $u_c = U - v_c$ where v_c is the velocity of vortex center referring to the cylinder. The longitudinal separation is calculated by $l = \frac{du_c}{US}$. The circulation, cir, was calculated by $\Gamma = \frac{2u_c l}{\tanh \frac{\pi k}{l}}$.

The computer program output is shown in Tables 3 and 4. Table 3 shows the radius of the vortex core. The dimensionless velocity components at the locations of $(\frac{x}{d}, \frac{y}{d})$ referring to free stream, $\frac{V_x d}{\Gamma_0}$ and $\frac{V_y d}{\Gamma_0}$, and the dimensionless velocity referring to the cylinder, $(U + u_c + V_x)\frac{d}{\Gamma_0}$, or FVX, are shown in Table 4. Figs 3 and 4 show the horizontal and vertical velocity components referring to the cylinder.

6. Discussion

6.1 The initiation of vortex shedding

Roshko (1954) has shown that the

Table 2. The experimental data

***TEST 10 *** DATE: 4/28/1988
CYLINDER DIAMETER = 1.25 IN
TEMPERATURE = 64.4 F
KINEMATIC VISCOSITY = 0.0000115 FT**2/SEC
FREE STREAM VELOCITY = 0.331 FT/SEC
REYNOLDS NUMBER = 2995.

X/D	F (1/S)	S	VC (FPS)	UC (FPS)	VC/U	H(FT)	L(FT)	CIR(F2/S)	STC (F2/S)	H/L	W/D
6.0	0.526	0.166	0.282	-0.049	0.852	0.183	0.535	-0.066	-0.074	0.343	3.800
8.0	0.563	0.178	0.276	-0.055	0.834	0.165	0.490	-0.068	-0.076	0.336	3.940
10.0	0.580	0.183	0.286	-0.045	0.864	0.177	0.493	-0.055	-0.063	0.359	3.880
12.0	0.526	0.166	0.294	-0.036	0.890	0.196	0.559	-0.051	-0.058	0.350	4.360
14.0	0.556	0.175	0.296	-0.034	0.896	0.242	0.533	-0.041	-0.052	0.453	5.000
16.0	0.541	0.170	0.301	-0.030	0.910	0.258	0.556	-0.037	-0.047	0.464	5.340
18.0	0.548	0.173	0.303	-0.028	0.917	0.335	0.553	-0.032	-0.043	0.607	5.860
20.0	0.548	0.173	0.305	-0.025	0.924	0.350	0.557	-0.029	-0.040	0.628	6.920
22.0	0.548	0.173	0.310	-0.021	0.938	0.348	0.566	-0.024	-0.033	0.615	7.020

Table 3 The radius of vortex cores

VORTEX NO.	1	2	3	4	5	6	7	8	9	10
CORE RADIUS (INCH)	0.0102	0.0125	0.0145	0.0162	0.0177	0.0192	0.0205	0.0217	0.0229	0.0240

Table 4. The velocity field of the viscous wake

X/D= 5.00 Y/D=	0.00	0.60	1.20	1.80	2.40	3.01	3.61	4.21	4.81	5.41	6.01	6.61
VX*D/GAMMA=	-0.173	-0.308	-0.042	0.226	0.098	0.058	0.040	0.031	0.025	0.021	0.018	0.016
VY*D/GAMMA=	-0.035	-0.023	-0.013	-0.006	0.000	0.003	0.005	0.006	0.007	0.007	0.007	0.006
FVX*D/GAMMA=	0.391	0.256	0.522	0.790	0.662	0.622	0.604	0.594	0.588	0.584	0.582	0.580
X/D= 6.29 Y/D=	0.00	0.60	1.20	1.80	2.40	3.01	3.61	4.21	4.81	5.41	6.01	6.61
VX*D/GAMMA=	-0.147	-0.125	-0.066	-0.006	0.019	0.024	0.024	0.023	0.021	0.019	0.017	0.016
VY*D/GAMMA=	-0.110	-0.117	-0.122	-0.091	-0.051	-0.026	-0.012	-0.005	-0.001	0.001	0.002	0.003
FVX*D/GAMMA=	0.417	0.438	0.498	0.557	0.582	0.588	0.588	0.586	0.584	0.583	0.581	0.580
X/D= 7.58 Y/D=	0.00	0.60	1.20	1.80	2.40	3.01	3.61	4.21	4.81	5.41	6.01	6.61
VX*D/GAMMA=	-0.196	-0.134	-0.085	-0.045	-0.016	0.001	0.010	0.015	0.016	0.016	0.016	0.015
VY*D/GAMMA=	-0.019	-0.017	-0.014	-0.011	-0.008	-0.006	-0.004	-0.003	-0.002	-0.001	0.000	0.001
FVX*D/GAMMA=	0.368	0.430	0.478	0.518	0.547	0.565	0.574	0.578	0.580	0.580	0.579	0.579
X/D= 8.87 Y/D=	0.00	0.60	1.20	1.80	2.40	3.01	3.61	4.21	4.81	5.41	6.01	6.61
VX*D/GAMMA=	-0.158	-0.138	-0.079	-0.018	0.008	0.016	0.017	0.017	0.016	0.016	0.015	0.014
VY*D/GAMMA=	0.069	0.083	0.095	0.070	0.036	0.015	0.005	0.001	-0.001	-0.001	-0.001	-0.001
FVX*D/GAMMA=	0.405	0.425	0.485	0.545	0.572	0.579	0.581	0.580	0.580	0.579	0.578	0.578
X/D=10.17 Y/D=	0.00	0.60	1.20	1.80	2.40	3.01	3.61	4.21	4.81	5.41	6.01	6.61
VX*D/GAMMA=	-0.203	-0.340	-0.073	0.199	0.076	0.040	0.026	0.020	0.017	0.015	0.014	0.013
VY*D/GAMMA=	-0.013	-0.012	-0.011	-0.010	-0.009	-0.008	-0.006	-0.005	-0.005	-0.004	-0.003	-0.003
FVX*D/GAMMA=	0.361	0.223	0.491	0.763	0.639	0.604	0.590	0.584	0.580	0.579	0.578	0.577
X/D=11.46 Y/D=	0.00	0.60	1.20	1.80	2.40	3.01	3.61	4.21	4.81	5.41	6.01	6.61
VX*D/GAMMA=	-0.163	-0.143	-0.084	-0.024	0.003	0.011	0.012	0.013	0.013	0.012	0.012	0.012
VY*D/GAMMA=	-0.097	-0.108	-0.117	-0.090	-0.053	-0.030	-0.018	-0.011	-0.008	-0.006	-0.005	-0.004
FVX*D/GAMMA=	0.401	0.420	0.480	0.540	0.567	0.574	0.576	0.576	0.576	0.576	0.576	0.575

X/D= 5.00 Y/D=	0.00	-0.60	-1.20	-1.80	-2.40	-3.01	-3.61	-4.21	-4.81	-5.41	-6.01	-6.61
VX*D/GAMMA=	-0.173	-0.120	-0.085	-0.059	-0.040	-0.028	-0.020	-0.016	-0.013	-0.011	-0.010	-0.009
VY*D/GAMMA=	-0.035	-0.045	-0.051	-0.051	-0.045	-0.038	-0.032	-0.027	-0.023	-0.020	-0.017	-0.015
FVX*D/GAMMA=	0.391	0.443	0.478	0.505	0.524	0.536	0.543	0.548	0.551	0.553	0.554	0.555
X/D= 6.29 Y/D=	0.00	-0.60	-1.20	-1.80	-2.40	-3.01	-3.61	-4.21	-4.81	-5.41	-6.01	-6.61
VX*D/GAMMA=	-0.147	-0.132	-0.079	-0.025	-0.003	0.000	-0.001	-0.003	-0.004	-0.005	-0.005	-0.005
VY*D/GAMMA=	-0.110	-0.126	-0.139	-0.113	-0.077	-0.052	-0.038	-0.030	-0.024	-0.021	-0.018	-0.016
FVX*D/GAMMA=	0.417	0.432	0.485	0.539	0.560	0.564	0.562	0.561	0.560	0.559	0.559	0.559
X/D= 7.58 Y/D=	0.00	-0.60	-1.20	-1.80	-2.40	-3.01	-3.61	-4.21	-4.81	-5.41	-6.01	-6.61
VX*D/GAMMA=	-0.196	-0.337	-0.073	0.196	0.069	0.031	0.015	0.007	0.003	0.000	-0.001	-0.002
VY*D/GAMMA=	-0.019	-0.022	-0.023	-0.024	-0.024	-0.023	-0.022	-0.021	-0.020	-0.018	-0.017	-0.016
FVX*D/GAMMA=	0.368	0.227	0.491	0.759	0.633	0.595	0.578	0.570	0.566	0.564	0.563	0.562
X/D= 8.87 Y/D=	0.00	-0.60	-1.20	-1.80	-2.40	-3.01	-3.61	-4.21	-4.81	-5.41	-6.01	-6.61
VX*D/GAMMA=	-0.158	-0.141	-0.084	-0.026	-0.001	0.004	0.005	0.004	0.002	0.001	0.001	0.000
VY*D/GAMMA=	0.069	0.080	0.089	0.062	0.026	0.004	-0.008	-0.013	-0.015	-0.015	-0.015	-0.014
FVX*D/GAMMA=	0.405	0.423	0.480	0.538	0.562	0.568	0.568	0.567	0.566	0.565	0.564	0.564
X/D=10.17 Y/D=	0.00	-0.60	-1.20	-1.80	-2.40	-3.01	-3.61	-4.21	-4.81	-5.41	-6.01	-6.61
VX*D/GAMMA=	-0.203	-0.143	-0.097	-0.059	-0.031	-0.014	-0.005	0.000	0.001	0.002	0.002	0.001
VY*D/GAMMA=	-0.013	-0.014	-0.015	-0.015	-0.016	-0.016	-0.016	-0.015	-0.015	-0.014	-0.014	-0.013
FVX*D/GAMMA=	0.361	0.420	0.466	0.505	0.533	0.550	0.559	0.563	0.565	0.565	0.565	0.565
X/D=11.46 Y/D=	0.00	-0.60	-1.20	-1.80	-2.40	-3.01	-3.61	-4.21	-4.81	-5.41	-6.01	-6.61
VX*D/GAMMA=	-0.163	-0.144	-0.087	-0.028	-0.002	0.005	0.006	0.005	0.004	0.004	0.003	0.003
VY*D/GAMMA=	-0.097	-0.109	-0.120	-0.094	-0.058	-0.036	-0.024	-0.019	-0.016	-0.014	-0.013	-0.013
FVX*D/GAMMA=	0.401	0.419	0.477	0.536	0.562	0.568	0.569	0.569	0.568	0.567	0.567	0.566

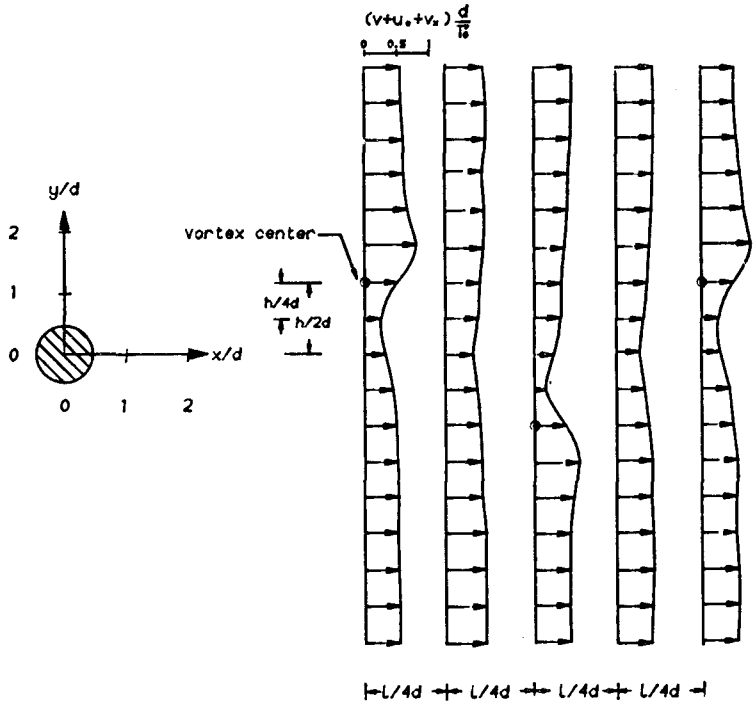

Figure 3. The horizontal velocity distribution of the viscous wake

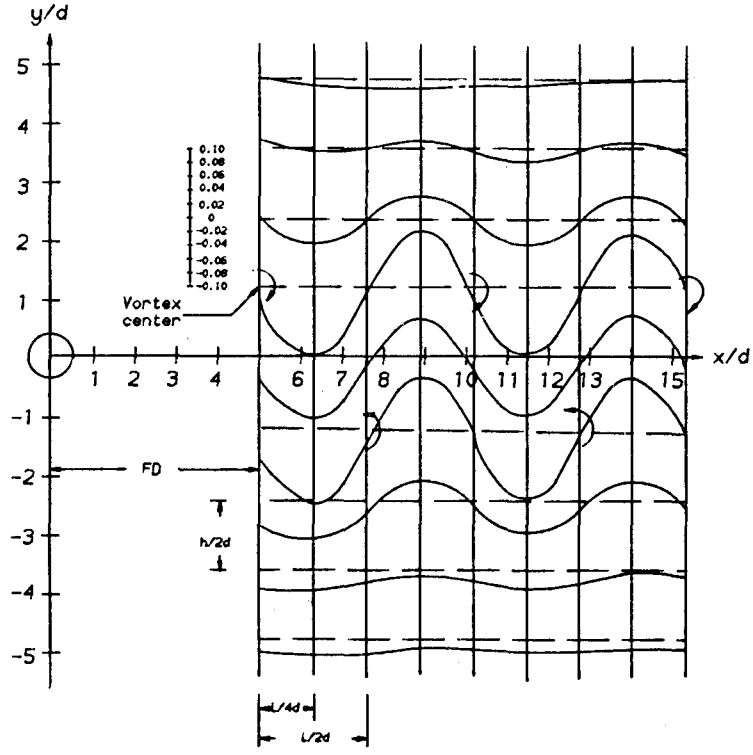

Figure 4. The vertical velocity distribution of the viscous wake

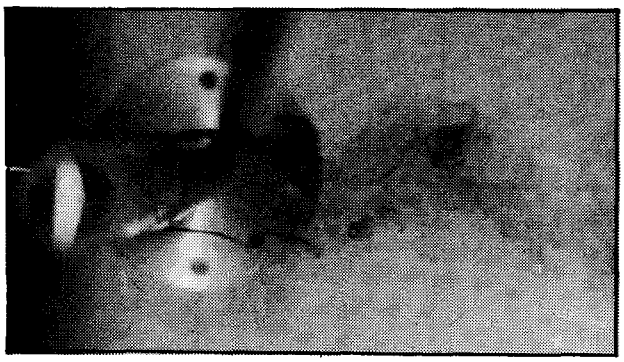

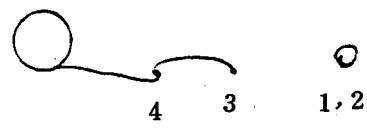

new secondary vortexes from separation of the cylinder

already combined from two secondary vortexes

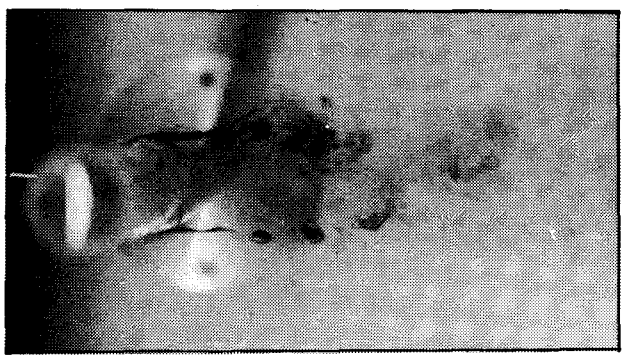

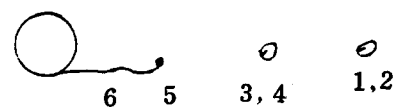

new secondary vortexes

two already combined vortexes will combine to a Strouhal vortex

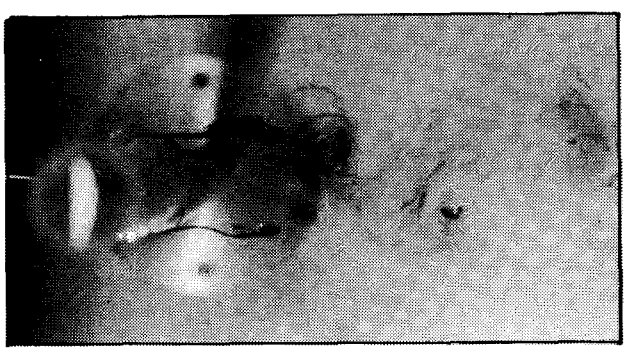

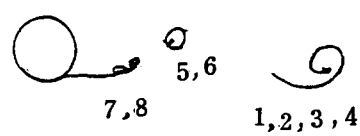

will combine as a Strouhal vortex

Strouhal vortex

Figure 5. The process of the combination from secondary vortexes to Strouhal vortex

Strouhal number remains almost constant at 0.2 in the Reynolds number range of $400 < \mathbf{R} < 3 \times 10^5$. Substituting $\mathbf{S} = 0.2$ into Eqs (3.6), (3.7), (3.11), and (3.12), yields

$$\frac{r_m^{(1)}}{d} = \frac{5}{\sqrt{\mathbf{R}}} \tag{6.1}$$

$$\frac{v_m^{(1)} d}{\Gamma_0} = 0.0224(\mathbf{R})^{\frac{1}{2}} \tag{6.2}$$

$$\frac{v_\theta^{(1)} d}{\Gamma_0} = \frac{1}{2\pi}\left(\frac{d}{r}\right)\left(1 - e^{-\frac{\mathbf{R}}{20}\left(\frac{r}{d}\right)^2}\right) \tag{6.3}$$

and

$$\frac{r_m^{(n)}}{d} = 5\sqrt{\frac{n}{\mathbf{R}}} \tag{6.4}$$

$$\frac{v_m^{(n)} d}{\Gamma_0} = 0.0224\left(\frac{\mathbf{R}}{n}\right)^{\frac{1}{2}} \tag{6.5}$$

$$\frac{v_\theta^{(n)} d}{\Gamma_0} = \frac{1}{2\pi}\left(\frac{d}{r}\right)\left(1 - e^{-\frac{\mathbf{R}}{20n}\left(\frac{r}{d}\right)^2}\right) \tag{6.6}$$

Eqs (6.1) to (6.6) can predict the core radius, the maximum velocity, and the tangential velocity of the first and the nth vortex.

From Eq. (6.1), in the Reynolds number range $400 < \mathbf{R} < 3 \times 10^5$, the first vortex behind the cylinder has the relation of

$$\frac{r_m^{(1)}}{d} = \frac{5}{\sqrt{\mathbf{R}}}$$

Since the laminar boundary layer thickness along a plate is (Daily and Harleman, 1966)

$$\frac{\delta}{x} = \frac{5}{\sqrt{\mathbf{R}_x}} \tag{6.7}$$

the $r_m^{(1)}$ and d are similar to the δ and x. This could be described as a relationship between the initiation of the vortex shedding and the boundary layer thickness. It coincides to the hypothesis of

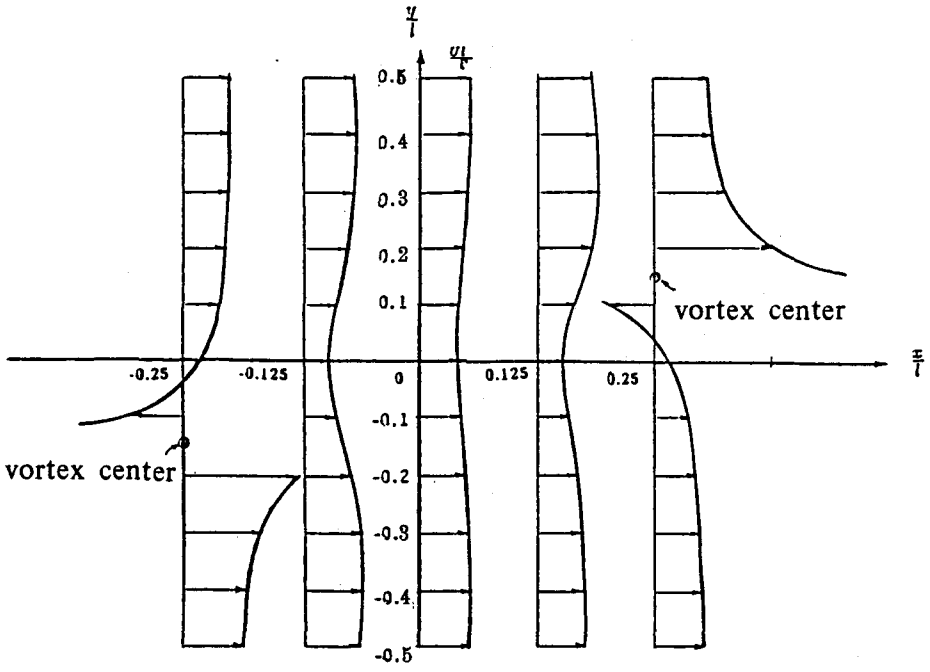

Figure 6. The horizontal velocity distribution of the potential wake

Wei and Smith (1986), that is "The most logical suggestion for origin of secondary vortexes is that they develop in the boundary layer separating from the cylinder."

Fig 5 shows three photo which were taken in the Albrook Laboratory, Washington State University. They show the process from the secondary vortexes to the Strouhal vortex. The Strouhal vortex is combined from four secondary vortexes. According to the area combination, the radius of the core of the Strouhal vortex is the diameter of the secondary vortex which is the boundary layer thickness.

6.2 The comparison of the velocity distribution between the viscous wake and the potential wake

Fig 6 shows the velocity distribution of the potential wake (Mih and Tseng, 1988). The only difference of Figs 3 and 6 is the velocity distributions at the core of the vortexes. This is coinciding to the viscous effect to the potential vortex that becomes a Rankine vortex.

References

Bloor, S.M. and J.H. Gerrard, "Measurements on Turbulent vortices in a Cylinder Wake," *Proceedings of the Royal Society of London, Serial A*, Vol. 294, 1966. pp. 319-342.

Daily, J.W. and D.R.F. Harleman, *Fluid Dynamics*, Addison-Wesley, 1966.

Hooker, S.G , "The Action of Viscosity in Increasing the Spacing Ratio of a Vortex Street," *Proceedings of the Royal Society of London*, Serial A, Vol. 154, 1936. pp. 67-89.

Karman, T. Von, and H. Rubach, "Uber den Medhanismus des Flussigkeits und Luftwiderstandes," *Physikalische Zeitschrift*, Vol. 13, No. 2, Jan. 1912 (English translation available from the National Aeronautics and Space Administration). pp. 49-59.

Lamb, H., *Hydrodynamics*, sixth edition, Cambridge University press, London, 1932.

Mih, W.C. and C.Y. Tseng "Velocity Field of Viscous Vortex Street in the Wake of a Cylinder," Unpublished proposal for doctoral dissertation, 1988.

Odgaard, A.J., "Free Surface Air Core Vortex," *Journal of Hydraulic Engineering*, American Society of Civil Engineers, Jul. 1986. pp. 610-620.

Oseen, C.W., *Hydrodynamik*, Leipzig, 1927, and *Ark. f. Mat., Astron. och Fys.*, Vol. 7, 1911. pp. 1-11.

Rankine, M.J., *A Manual of Applied Mechanics*, Griffin, London, 1858.

Roshko, A., *On the Development of Turbulent Wakes from Vortex Streets*, National Advisory Committee for Aeronautics (NACA) Report 1191, 1954. (Technical Note, 1953.) pp. 801-825.

Schaefer, J.W. and S. Eskinazi, "An Analysis of the Vortex Street Generated in a Viscous Fluid," *Journal of Fluid Mechanics*, Vol. 6, 1959. pp. 241-260.

Strouhal, V. "Uber eine Besondere Art de Tonerregung," *Annual Physik and Chemie*, Neue Folge, Bd. 5, Heft 10, Oct. 1878. pp. 216-251.

Wei, T. and C.R, Smith, "Secondary vortices in the wake of circular cylinder," *Journal of Fluid Mechanics*, Vol. 169, 1986. pp. 513-533.